Vertical and Horizontal Ridge Augmentation Using Customized Three-Dimensionally Printed Polycaprolactone Mesh in Atrophic Posterior Maxillae: A Case Report

Jin-Young Park[1]
Su-Hee Jeon[1]
Joo-Yeon Lee[1]
Ji-Man Park[2*]
Jae-Kook Cha[1*]

Polycaprolactone has exhibited expediency as a biomaterial for bone regenerative procedures preclinically. The present report of the 2 clinical cases in the posterior maxilla is the first to describe clinical application of a customized 3D-printed polycaprolactone mesh for alveolar ridge augmentation. Two patients needing extensive ridge augmentation procedures for dental implant therapy were selected. Polycaprolactone meshes were virtually designed, 3D printed, and applied in combination with a xenogeneic bone substitute. Cone-beam computerized tomography was taken preoperatively, immediately after the surgery, and 1.5–2 years after the delivery of implant prostheses. The serial cone-beam computerized tomography images were superimposed to measure the augmented height and width at 1-mm increments from the implant platform to 3 mm apically. After 2 years, the mean [maximum, minimum] bone gain was 6.05 [8.64, 2.85] mm vertically and 7.77 [10.03, 6.18] mm horizontally at 1 mm below the implant platform. From immediately postoperative to 2 years, there was 14% reduction of augmented ridged height and 24% reduction of augmented width at 1 mm below the platform. All implants placed in augmented sites were successfully maintained until 2 years. The customized polycaprolactone mesh might be a viable material for ridge augmentation in the atrophic posterior maxilla. This needs to be confirmed through randomized controlled clinical trials in future studies.

Key Words: 3D printing, polycaprolactone, ridge augmentation

Introduction

Guided bone regeneration (GBR) has been considered as a reliable technique for horizontal and vertical ridge augmentation in the damaged and atrophic ridge.[1,2] Though various types of membranes have been evaluated in previous studies, among them, the resorbable collagen membrane has been regarded as the standard of care in clinical situations.[3,4] However, the resorbable collagen membrane lacks mechanical stability for optimal space maintenance, and this is a prerequisite for successful bone regeneration.[5–7] Moreover, a ready-made collagen membrane needs to be cut and shaped according to the defect morphology before application, and this requires an operator's skill and time. For these reasons, there has been an emerging need for patient-specific membranes that can overcome the shortcomings of the conventional, ready-made resorbable membranes.

Recently, with the development of computer-aided design (CAD) and manufacturing technologies, it became possible to fabricate a customized membrane based on cone-beam computerized tomography (CBCT). Previous studies reported that the customized 3-dimensional printed titanium mesh could be used for GBR.[8,9] It has been described that the individualized 3D-printed titanium mesh can be safely and successfully used in ridge augmentation showing reliable clinical outcomes in terms of hard tissue generation. Another randomized clinical study compared the performance of customized titanium mesh to the conventional titanium mesh in GBR and showed that the customized mesh was more effective against postoperative infection and mucosal rupture.[10] Because the virtual design was carried out preoperatively for customized titanium mesh, it could be possible to make the edges of the mesh round and blunt, which leads to less soft tissue trauma and wound dehiscence.[9] However, despite the customization of the titanium mesh, the rate of exposure remains high, ranging from 21% to 31% according to recent clinical studies.[10,11]

Therefore, there has been much interest on other biomaterials with good biocompatibility and space maintenance properties. Polycaprolactone (PCL)-based synthetic mesh is a biocompatible material with a slow degradation rate that has sufficient strength to maintain space.[12] Furthermore, because PCL can be 3D printed, it can be customized to fit each defect.

[1] Department of Periodontology, Research Institute for Periodontal Regeneration, Yonsei University College of Dentistry, Seoul, Korea. 50-1 Yonsei-Ro Shinchon Dong Seodaemun-Gu KOREA, REPUBLIC OF Seoul Seoul 03799.
[2] Department of Prosthodontics and Dental Research Institute, Seoul National University School of Dentistry, 101 Daehak-ro, Jongno-gu, Seoul 03080, Republic of Korea.
* *Corresponding authors*, e-mail: chajaekook@yuhs.ac; jimarn@gmail.com
https://doi.org/10.1563/aaid-joi-D-22-00007

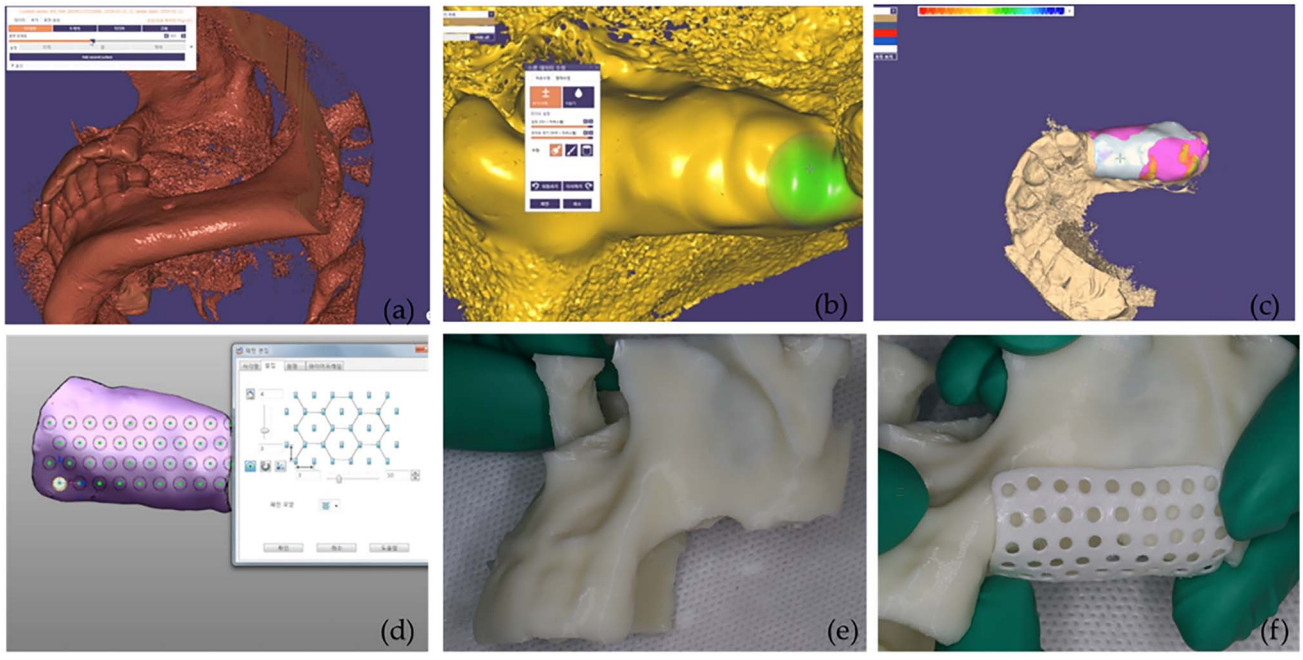

Figure 1. Design process of patient-specific customized membrane showing (a) 3D segmentation, (b) virtual bone augmentation, (c) membrane outline establishment and shape adjustment, (d) pore design, and (e and f) 3D printed rapid prototyping model and polycaprolactone mesh.

It has been shown that a synthetic, 3D-printed membrane could enhance bone augmentation compared with the titanium mesh preclinically.[13] However, to the best of our knowledge, there have been no clinical reports on the use of PCL mesh for GBR. Therefore, the aim of the current study was to evaluate the clinical feasibility and performance of customized, 3D-printed PCL mesh for GBR in the severely atrophic ridge.

Materials and Methods

Study design

Two participants were included in this study who had combined vertical and horizontal ridge deficiencies according to the Seibert classification.[14] They were treated by 2 different specialists in periodontics and implant surgery at the department of periodontology of Yonsei University Dental Hospital between 2019 and 2020. This study was conducted in accordance with the Declaration of Helsinki. The treatment procedure was approved by the institutional review board of Yonsei University Dental Hospital (approval no. 2021-0072), which abides by the good clinical practice guidelines and the regulatory requirements.

Design and fabrication of the PCL mesh

For the design of customized PCL mesh, the digital imaging and communication in medicine data from the CBCT imaging was converted into a stereolithographic file with a 3D segmentation software module (DICOM Viewer, exocad GmbH, Darmstadt, Germany) (Figure 1a). The position of the implants was virtually planned using implant planning software (Implant studio, 3shape, Copenhagen, Denmark). The 3D shape of the patient-specific mesh was designed using dental CAD (Exocad GmbH, Darmstadt, Germany) and a universal CAD software program (PowerShape, Autodesk Inc, San Rafael, CA). The defects were virtually augmented to form an ideal ridge shape on which the PCL mesh was designed (Figure 1b and c). The final design, including small pores, was completed using universal CAD (Figure 1d).

The completed design was transferred to the manufacturing practice facility (T&R Biofab, Seoul, Korea) approved by the ministry of food and drug safety. The mesh design was converted into printing path data for a preprocessing process through an algorithm optimized for a microextrusion-based 3D printer (3D Bioprinter; T&R Biofab, Siheung, South Korea). A medical-grade PCL material (Evonik Industry, Pharma Polymers, Essen, Germany) was used to create the PCL mesh. In brief, the operating mechanism of the 3D bioprinter was based on discharging the PCL in its molten state by maintaining the PCL-mounted syringe at 110°C. The thickness of printed PCL mesh was 0.5 mm. The completed mesh was sterilized with gamma rays, sealed, and delivered back to the hospital (Figure 1e and f).

Case I

A 60-year-old male patient was presented with advanced periodontitis and peri-implantitis at the upper left posterior region. The 2 upper left premolars along with 2 dental implants at the molar sites were extracted. A baseline CBCT (T0) was taken 6 months after the extraction (Figure 2). A combined vertical and horizontal alveolar bone deficiency could be seen on the CBCT imaging. Because it was difficult to place the implants in ideal positions, staged GBR was planned in which a customized PCL mesh was to be applied for the GBR initially and then followed by a healing period and placement of 2 implants at the upper left first premolar and first molar sites.

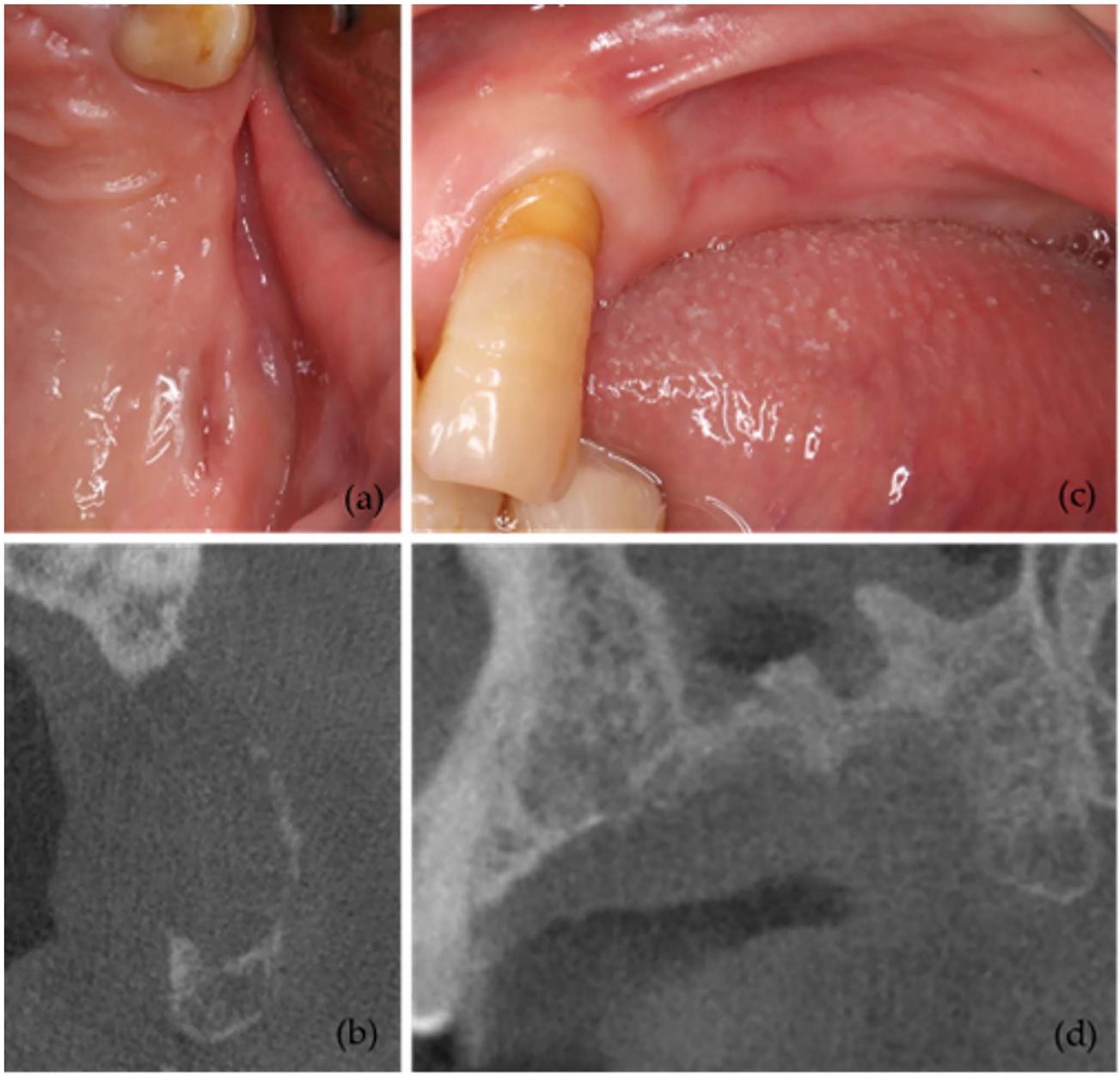

Figure 2. Case I: Preoperative clinical photos and cone-beam computerized tomography. (a and b) Occlusal view and (c and d) lateral view.

Local anesthesia was performed using lidocaine hydrochloride 1:100 000 with 2% epinephrine (Huons, Seongnam, Korea). After a midcrestal incision and a vertical incision on the mesial line angle of the adjacent tooth, a full thickness flap was elevated (Figure 3a). The PCL mesh was fixated using a bone tack (Membrane Pin, Dentium, Suwon, Korea) after grafting 0.5 g of demineralized bovine bone mineral with 10% collagen (Bio-Oss collagen, Geistlich Pharma AG, Wolhusen, Switzerland) to the defect site. Through the holes of the mesh, 0.5 g of xenogeneic bone substitute particles (Bio-Oss, Geistlich) were additionally applied (Figure 3b and c). After the flap advancement, primary closure was achieved by a combination of the vertical and horizontal mattress and interrupted sutures using 4-0 absorbable monofilament (Monosyn, B Braun, Melsungen, Germany) (Figure 3d). A second CBCT was taken immediately after the surgery (T1). Oral antibiotics (amoxicillin and clavulanic acid, 1.5 g per day) and a nonsteroidal anti-inflammatory drug (ibuprofen, 0.8 g per day) were prescribed for 7 days. The patient was instructed to rinse with 0.2% chlorhexidine twice a day for 10 days and apply ice packs to the surgical site for 48 hours. The sutures were removed 10 days after the surgery. No adverse reactions or complications were observed up to 6 months postoperatively (Figure 3e and f).

At reentry after 6 months, the PCL mesh was maintained without resorption or deformation. The fixation pins were removed along with the PCL mesh (Figure 4a and b). Two bone-level implants (Superline III, Dentium, Seoul, South Korea) were placed at the first premolar (Ø = 4.5 mm, length = 8 mm) and

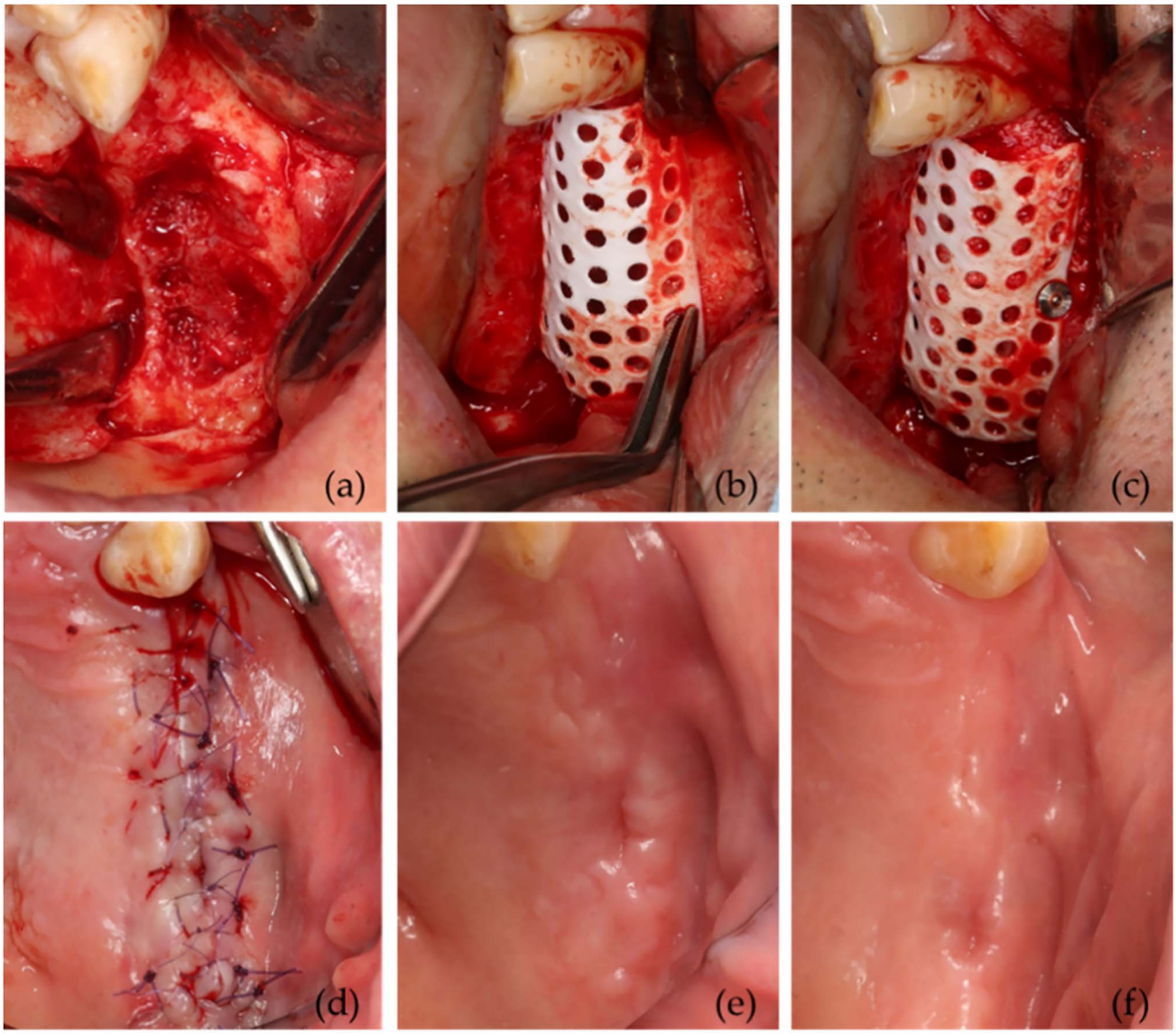

Figure 3. Case I: Guided bone regeneration procedure with customized polycaprolactone membrane, Mx. Lt. (a) Preop defect, (b) polycaprolactone membrane application with particle xenograft, (c) membrane fixation, (d) primary closure, (e) 1.5 months after GBR, and (f) 5 months after GBR.

molar (Ø = 5.0 mm, length = 8 mm) areas. Primary stability of 50 N was obtained for both implants; therefore, healing abutments were connected (Figure 4c and d). At 6 months after implant placement, an implant stability meter (Anycheck, Neobiotech, Seoul, Korea)[15] revealed implant stability test values of 78 and 82 for the 2 implants on upper left first premolar and first molar areas, respectively, and these were sufficient for loading of implants. Thence, the implant prosthesis was delivered. A third CBCT (T2) was taken at 2 years after ridge augmentation.

Case II

A 65-year-old female was presented with advanced periodontitis in the upper right region. The first and second maxillary molars were extracted, and baseline CBCT was taken 3.5 months after the extraction. A combined vertical and horizontal alveolar bone deficiency was observed (Figure 5b and d). Placement of 2 implants with simultaneous ridge augmentation and maxillary sinus graft via lateral window was planned.

The design and fabrication of customized PCL mesh was as described above (Figure 5e and f). Under local anesthesia, midcrestal and vertical incisions were made, and full thickness mucoperiosteal flaps were elevated. A lateral window to the maxillary sinus was prepared using a piezoelectric device (Piezosurgery, Mectron, Carasco, Italy), and after careful elevation of the Schneiderian membrane, deproteinized porcine bone mineral (The Graft, Purgo, Seoul, South Korea) was grafted. Two bone-level implants (Superline III, Dentium; Ø = 5.0, length = 8 mm) were placed using a fully guided surgical template, and 20 N of primary stability was achieved. Cover screws

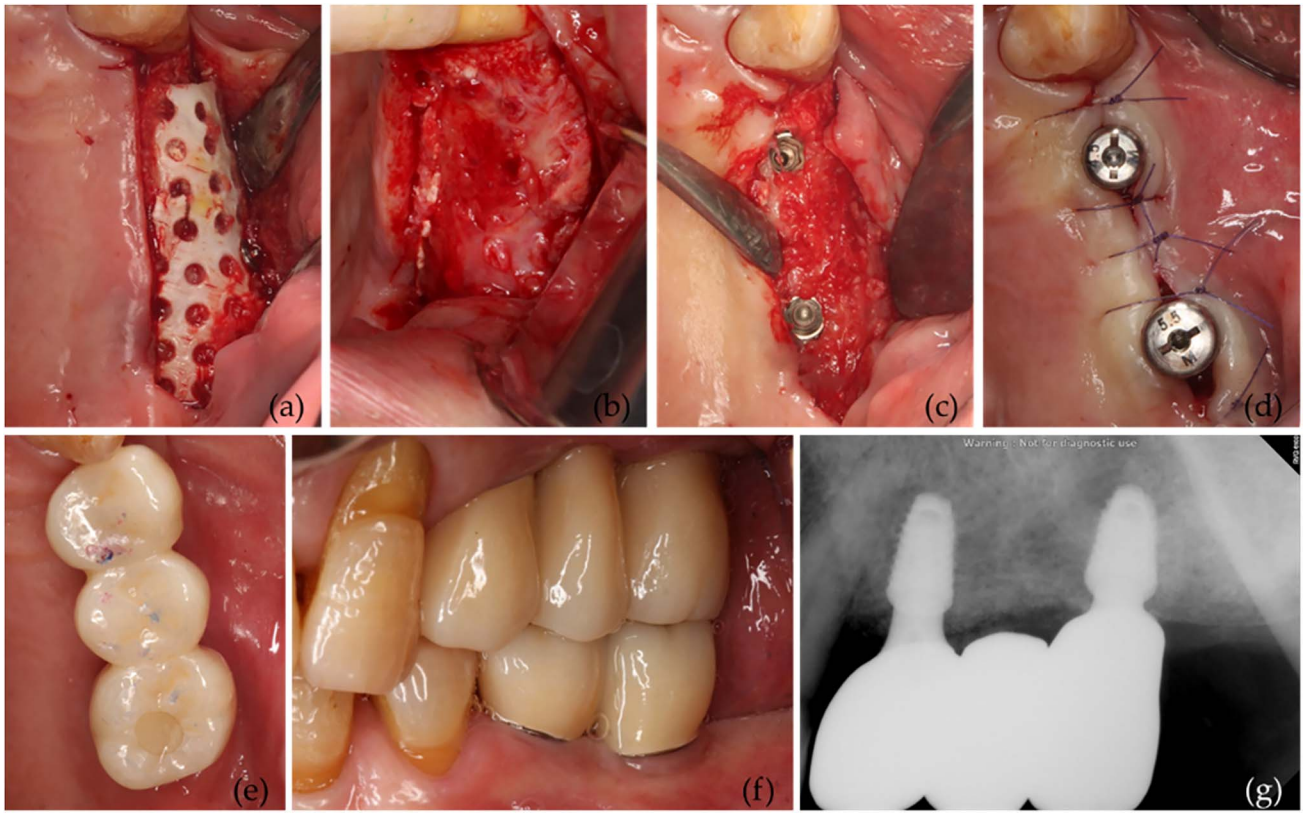

Figure 4. Case I: Implant placement. (a) Incision and flap elevation, (b) polycaprolactone membrane removal, (c) fixture installation (i24: 4.5 × 8 mm/50N, i26: 5.0 × 8 mm/50N), (d) primary closure, (e and f) prosthodontics treatment, and (g) periapical radiographs after treatment.

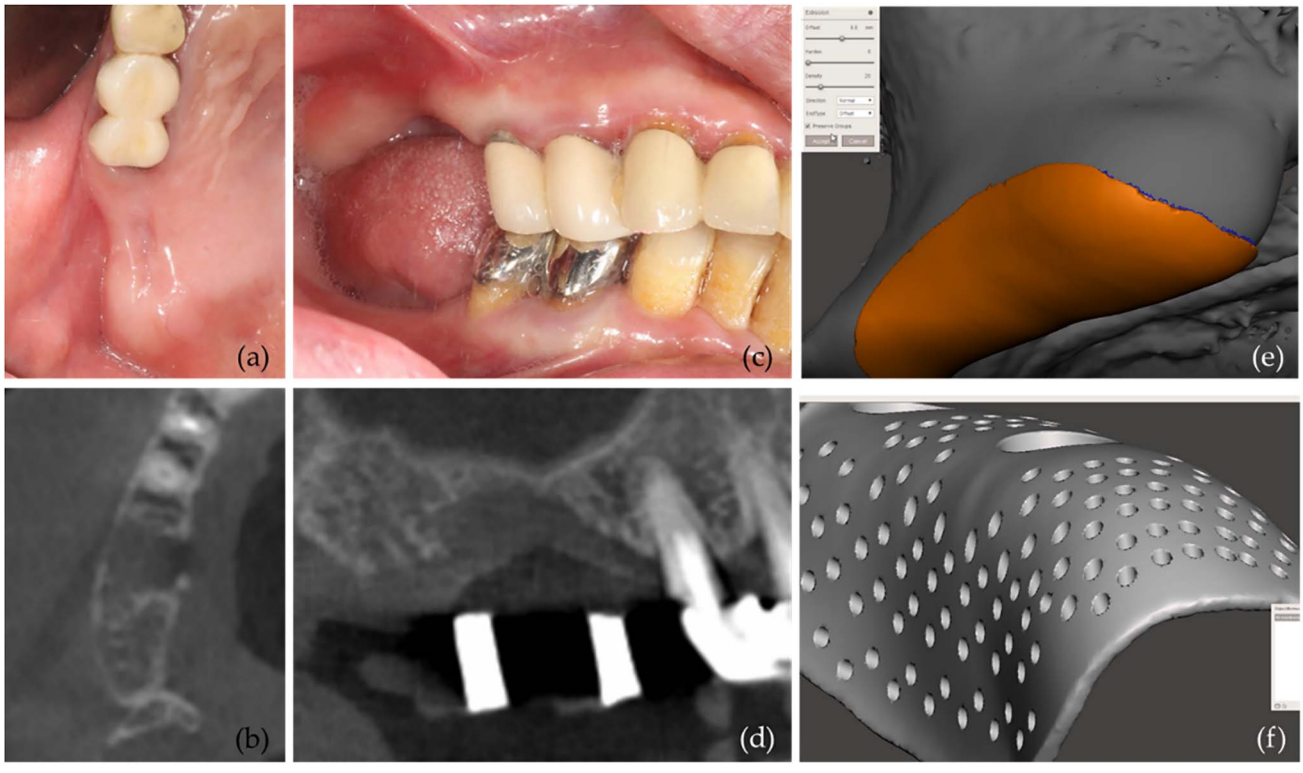

Figure 5. Case II: Preoperative clinical photos and cone beam computerized tomography. (a and b) Occlusal view; (c and d) lateral view, design process of patient-specific customized mesh; (e) virtual bone augmentation; and (f) design of polycaprolactone mesh.

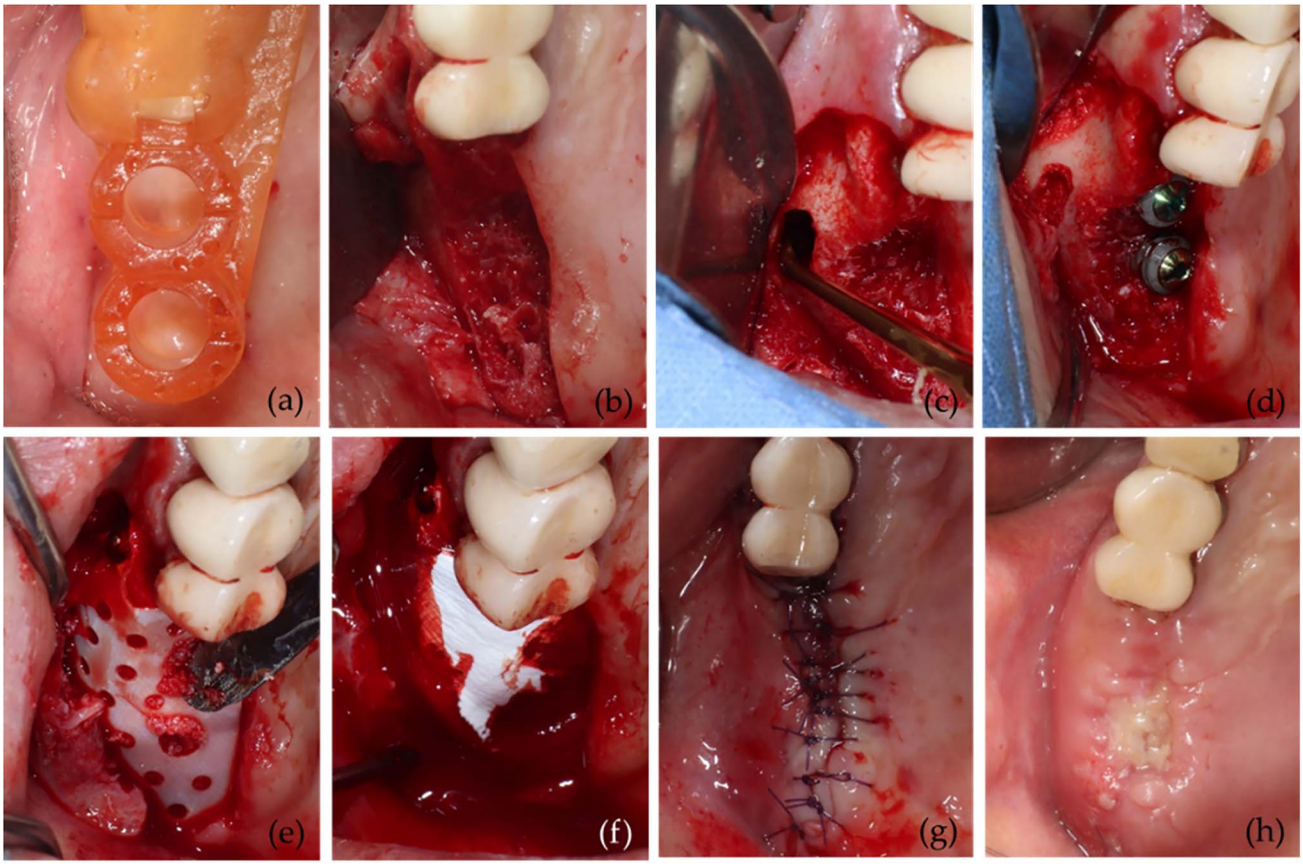

Figure 6. Case II: GBR and sinus graft with simultaneous implant placement. (a) Surgical guide placement, (b) incision and flap elevation, (c) sinus graft with lateral approach, (d) fixture installation (i16, 17: 5.0 × 10 mm, 20N), (e) polycaprolactone mesh application with particle xenograft, (f) collagen membrane application, (g) primary closure, and (h) stitch out.

were connected to the fixtures (Figure 6d). Then, 0.5 g of deproteinized porcine bone mineral was applied to the defect site, and the PCL mesh was placed and fixed with a fixation pin (Membrane Pin, Dentium); 0.5 g of deproteinized porcine bone mineral was applied additionally into the remaining space through the mesh hole (Figure 6e), and a resorbable collagen membrane (Bio-Gide, Geistlich) was additionally covered over the PCL mesh (Figure 6f). The buccal flap was advanced to achieve primary closure, and a combination of mattress and interrupted sutures were utilized (Figure 6g). The same protocol for postoperative care was taken as for case I. A second CBCT (T1) was taken immediately after the surgery. A wound dehiscence was observed at 2 weeks after the surgery (Figure 6h). The exposure site remained clear of infection under daily dressing and strict oral hygiene. Over the 4-month follow-up, the exposed site became re-epithelialized by secondary healing (Figure 7a).

The reentry was performed at 4 months postoperatively. Once the fixation pin was removed, the PCL mesh could be easily separated from the augmented tissue. Formation of new bone could be observed around the fixtures and covering the fixture threads. Augmented contour of the alveolar ridge appeared to be well-maintained (Figure 7b). Healing abutments were connected and flaps sutured. A third CBCT was taken 1.5 years postoperatively (T2).

Radiographic analysis

The augmented sites from the 2 cases were evaluated by superimposing the consecutive CBCTs taken preoperatively (T0), immediately after surgery (T1), and 1.5–2 years after surgery (T2). Superimposition and linear analyses were carried out using a 3D analytic software (OnDemand3D, Cybermed, Seoul, South Korea), and CBCT data from each period was loaded onto the software and superimposed using teeth as reference points. The height of augmented bone was measured along the long axis of each implant (Figure 8a), and the measurement was performed from the original bone bed at T0 to the augmented bone crest at T1 and T2. The augmented bone width was measured at levels 1, 2, and 3 mm (H1, H2, and H3, respectively) apical from the implant platform (Figure 8b), and the measurements were made from the buccal surface of the implant fixture to the augmented buccal bone crest at T1 and T2.

Results

Clinical evaluation

In both cases, the patient visited the clinic every 3–6 months for supportive periodontal therapy after completion of implant-fixed prosthetic treatment. During the 2-year follow-up period, no

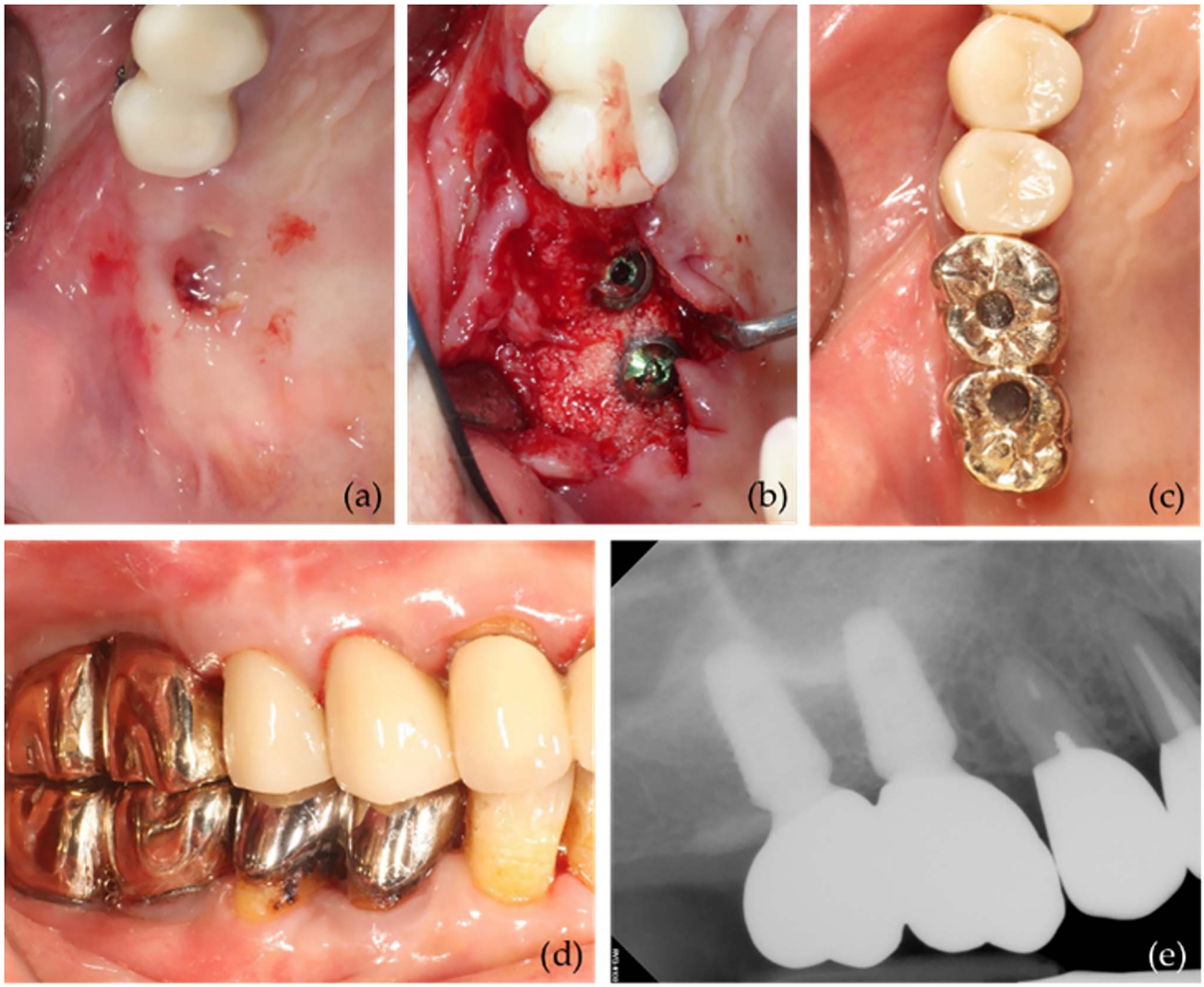

Figure 7. Case II: Implant second surgery and prosthodontic treatment. (a) Preop, (b) flap elevation, (c and d) prosthodontic treatment, and (e) periapical radiographs after treatment.

adverse events or abnormal findings were detected at the augmented sites (Figures 4 and 7).

Radiographic evaluation

Overall, the mean augmented height of the measured sites was 7.26 mm at T1, and this was reduced to 6.05 mm at T2. The mean augmented widths at T1 were 10.64, 10.28, and 10.85 mm at H1, H2, and H3, respectively; these were reduced to 7.77, 8.38, and 9.24 mm, respectively. The vertical shrinkage during the healing period up to 2 years was less than the horizontal shrinkage at H1 (14% and 24%, respectively).

In case I, the mean augmented height at T1 was 10.62 mm, and this became reduced to 8.58 mm at T2. The mean augmented widths at T1 were 13.68, 12.62, and 11.82 mm at H1, H2, and H3, respectively; these were reduced to 9.01, 9.84, and 9.94 mm, respectively (Figure 9 and Table 1).

In case II, the mean augmented height of the measured sites was 3.91 mm at T1, and this was reduced to 3.52 mm at T2. The mean augmented widths at T1 were 7.6, 7.95, and 8.91 mm at H1, H2, and H3, respectively; these were reduced to 6.54, 6.93, and 7.84 mm, respectively (Figure 10 and Table 2).

Discussion

To the authors' knowledge, the present study is the first clinical report on the use of PCL mesh for ridge augmentation. The PCL mesh demonstrated some beneficial characteristics as a barrier membrane for GBR. In the challenging situation of the posterior maxilla, the vertically and horizontally augmented ridges using the 3D-printed PCL mesh were well maintained for 2 years along with the successfully placed implants.

There have been numerous preclinical studies demonstrating the potential expediency of PCL as a biomaterial for GBR.[16–19] Although various synthetic polymer materials have been investigated in different preclinical models, biocompatibility of those materials has been the major hurdle prior to clinical application. However, recent in vivo studies using PCL have

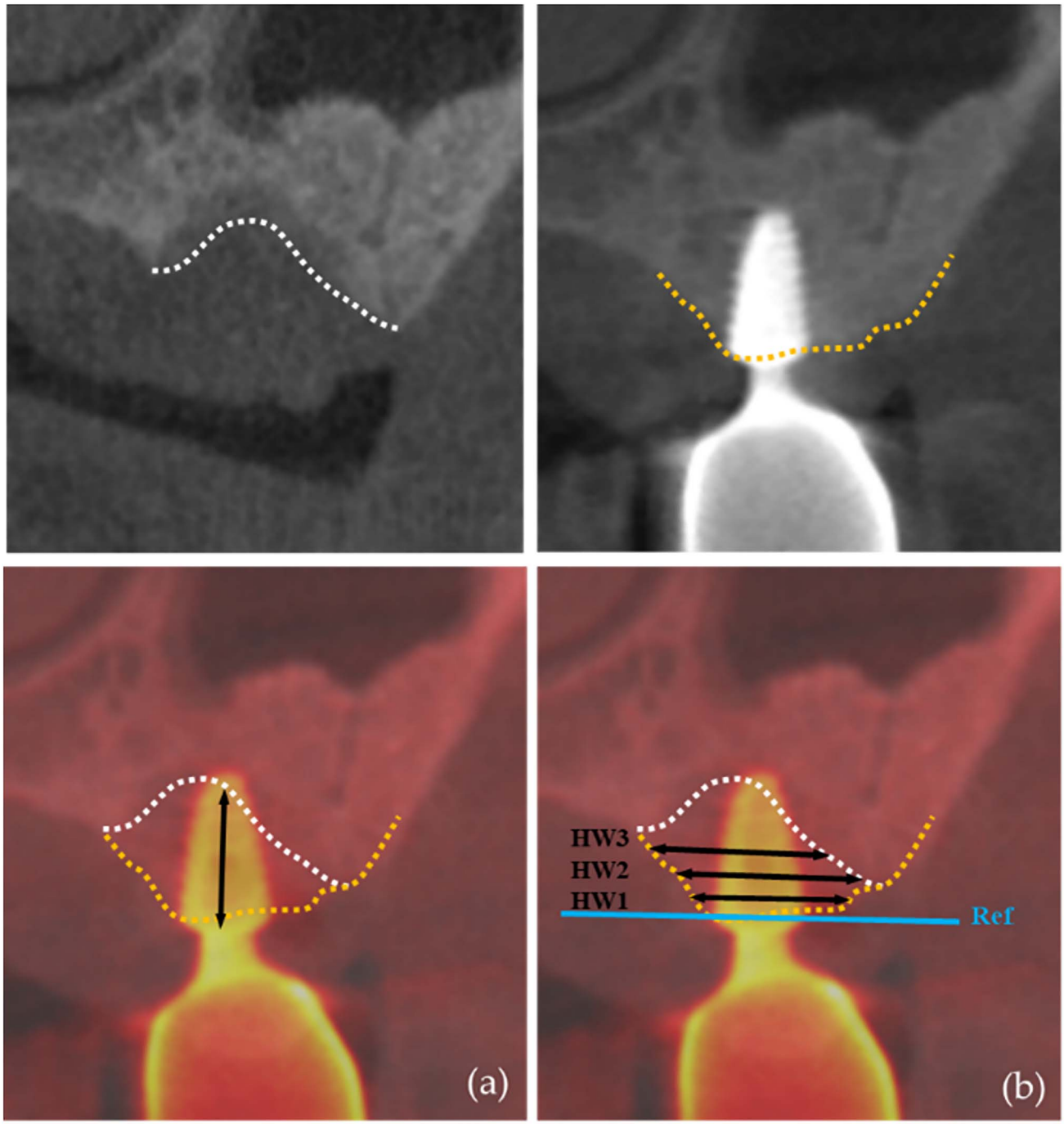

Figure 8. Radiographic measurement. Preoperative crestal margin (white dotted) and postoperative crestal margin (yellow dotted) in middle of cross-sectional view of implant fixture. (a) Vertical measurement (black line) and (b) horizontal measurement at the level of 1, 2, and 3 mm (black line) from the reference line, which was the shoulder of the implant fixture.

demonstrated not only minimal to no foreign body reaction when applied as a barrier membrane or scaffold but also de novo deposition of newly formed bone onto the biomaterial.[17,20] Other in vitro studies have also investigated surface characteristics and porosity of PCL for osteogenic cellular activity and expression growth factors in which successful outcomes have been demonstrated.[21] Therefore, combined with the controllable characteristics of the material, including the shape, porosity, and chemical composition during fabrication, PCL has great potential to be utilized for bone tissue engineering.

In this study, PCL mesh was applied as a barrier membrane for GBR in the atrophied maxilla. The posterior maxilla can be a challenging situation for ridge augmentation due to the poor bone quality, presence of the maxillary sinus, and the unfavorable defect configuration that can occur from the loss of maxillary tuberosity. Although the maxillary tuberosity

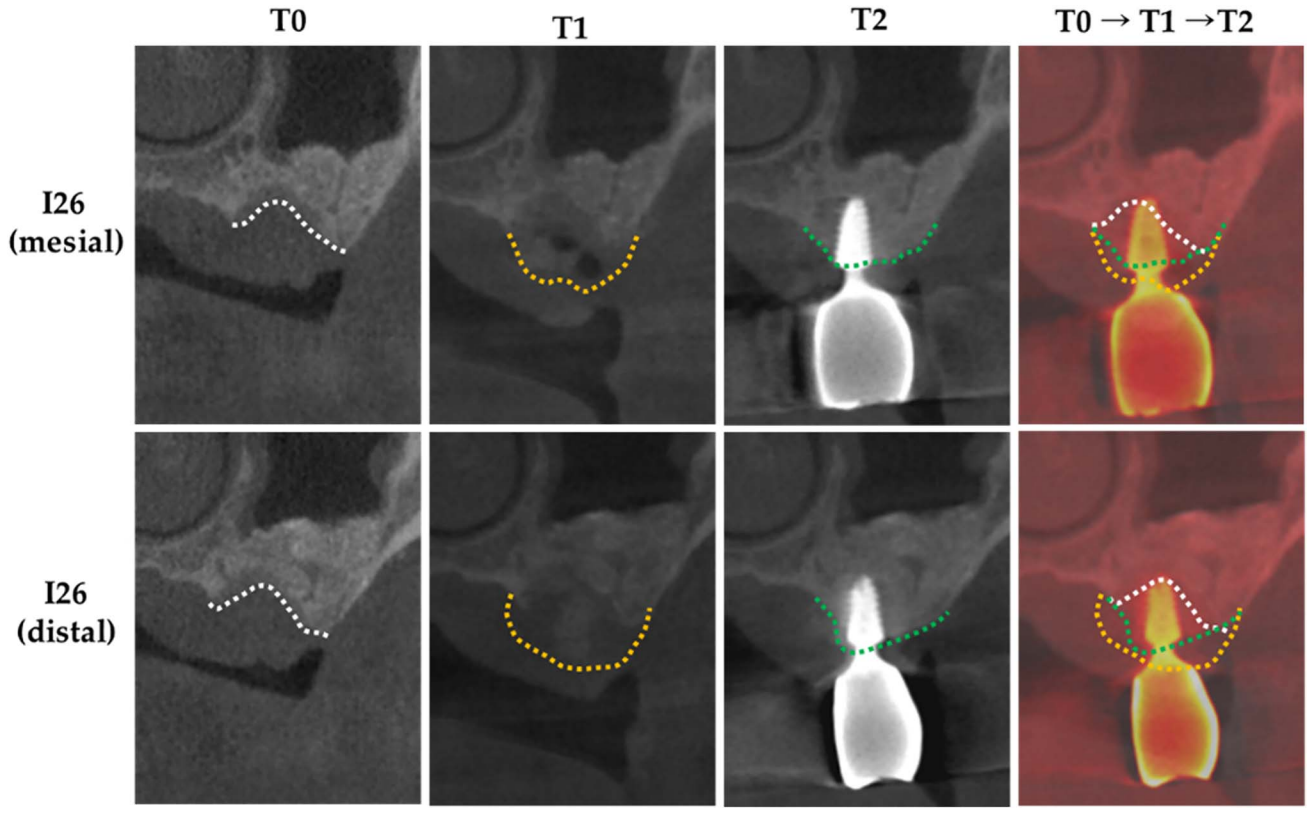

Figure 9. Cross-sectional images of case I; T0: preoperative; T1: immediately after surgery; T2: 2 years after surgery; preoperative crestal bone margin (black dotted line); augmented bone margin immediately after surgery (yellow dotted line); augmented bone margin 2 years after surgery (green line).

was preserved in both cases, providing a posterior support of the graft materials, the 2 cases exhibited sizeable defects, including vertical deficiency. The major issue in this circumstance was the provision of space and maintenance of stability over the prolonged healing period required for bone formation. Traditionally, more invasive treatment approaches had been advocated, such as block bone graft and distraction osteogenesis. However, a recent meta-analysis has demonstrated that comparable vertical bone gain can be achieved using the GBR technique with a considerably lower complication rate. In that study, the weighted mean vertical gain for GBR was 4.18 mm. Considering the mean vertical gain of 6.05 mm in this study, the amount of vertical augmentation in this study was not inferior to that of the literature. In this respect, PCL mesh might be a viable solution for the augmentation of the severely atrophied ridge.

Table 1

Radiographic measurements of case I

Location	T0* → T1†§	T0* → T2‡|	Amount of Reduction, %
I26 (mesial)			
Vertical	10.31	8.64	16.2
Horizontal			
1 mm	14.21	10.03	29.42
2 mm	11.98	11.56	3.50
3 mm	11.14	10.31	7.45
I26 (distal)			
Vertical	10.92	8.52	21.98
Horizontal			
1 mm	13.14	7.98	39.27
2 mm	13.25	8.11	38.79
3 mm	12.50	9.56	23.52

*T0: preoperation.
†T1: immediately after surgery.
‡T2: 2 years after surgery.
§T0 → T1: change of augmented bone height and width from preoperation to immediately after surgery.
|T0 → T2: change of augmented bone height and width from preoperation to 2 years after surgery.

In this study, the PCL mesh was unresorbed up to 6 months. Although PCL has been regarded as a bioresorbable material in previous studies, little is known about the degradation kinetics within the vital surroundings due to the extremely slow degradation rate. Preclinical studies also have shown that PCL membranes and scaffolds were unresorbed in animal models such as rabbit calvarial defects and dog alveolar defects up to 8 weeks.[17,20] In a study in rats, subdermal capsules of radioactively labeled "PCL" were maintained up to 30 months. Once resorbed, however, no traces of the labeled PCL accumulated in the body, confirming the safety of the material.[12] It has been shown that the resorption rate may vary according to the pore size of the biomaterial as well as the proportion of β-TCP content when used as a mixture.[13,18] The effect of the longevity of barrier function on the outcome of GBR can be

Table 2

Radiographic measurements of case II

Location	T0* → T1†§	T0* → T2‡|	Amount of Reduction, %
I16			
Vertical	2.90	2.85	1.72
Horizontal			
1 mm	7.46	6.89	7.64
2 mm	7.11	6.41	2.95
3 mm	none	none	
I17			
Vertical	4.92	4.19	14.84
Horizontal			
1 mm	7.73	6.18	20.05
2 mm	8.79	7.45	15.24
3 mm	8.91	7.84	12.01

*T0: preoperation.
†T1: immediately after surgery.
‡T2: 1.5 years after surgery.
§T0 → T1: change of augmented bone height and width from preoperation to immediately after surgery.
|T0 → T2: change of augmented bone height and width from preoperation to 1.5 years after surgery.

debatable because of the transition of the conventional GBR concept using nonresorbable membranes to the more frequently used collagen membranes today.[22] It might be possible that we can take advantage of the controllable resorption characteristics of PCL to optimize bone regeneration in future studies.

Because the PCL membrane was applied in the form of a mesh, it might be compared with the titanium mesh. Previous studies have shown that, on a healed ridge augmented using titanium mesh, thickened layers of connective tissue surrounded the mesh structures, and these may appear as a dense fibrous layer covering the augmented bone.[23–25] Similar histological appearances have been reported with the PCL membrane in which the materials were surrounded by dense connective tissue after 8 weeks of healing in the rabbit calvarial defect model.[16] These histological descriptions may suggest that PCL exhibits good tissue integration and biocompatibility. Because the collagenous matrix provides the foundation for the deposition of bone, it is conceivable that integration of mineralized tissues might occur in these areas after longer healing periods.

Because the PCL membrane can be 3D printed, there is a great advantage that numerous conditions can be controlled, including pore size, chemical composition, and loading of signaling molecules. Furthermore, it is possible to construct creative customized shapes to optimize the augmentation procedure. For example, PCL could be 3D printed as customized plates with structural rigidity to be used as supporting blocks for reconstruction. In this respect, PCL as a biomaterial appears to have a promising potential for bone regeneration.

There were some limitations to this study. Because this is a presentation of 2 cases, it is difficult to draw a conclusion about the efficacy of the PCL mesh from the results of this study alone. Nevertheless, the detailed descriptions of the preparation of the PCL mesh and the surgical procedures can be taken into consideration. Moreover, it is important to acknowledge that the successful outcome of the bone augmentation procedures does not depend exclusively on the material selection but also on appropriate case selection and meticulous management of the mucoperiosteal flaps during surgery.

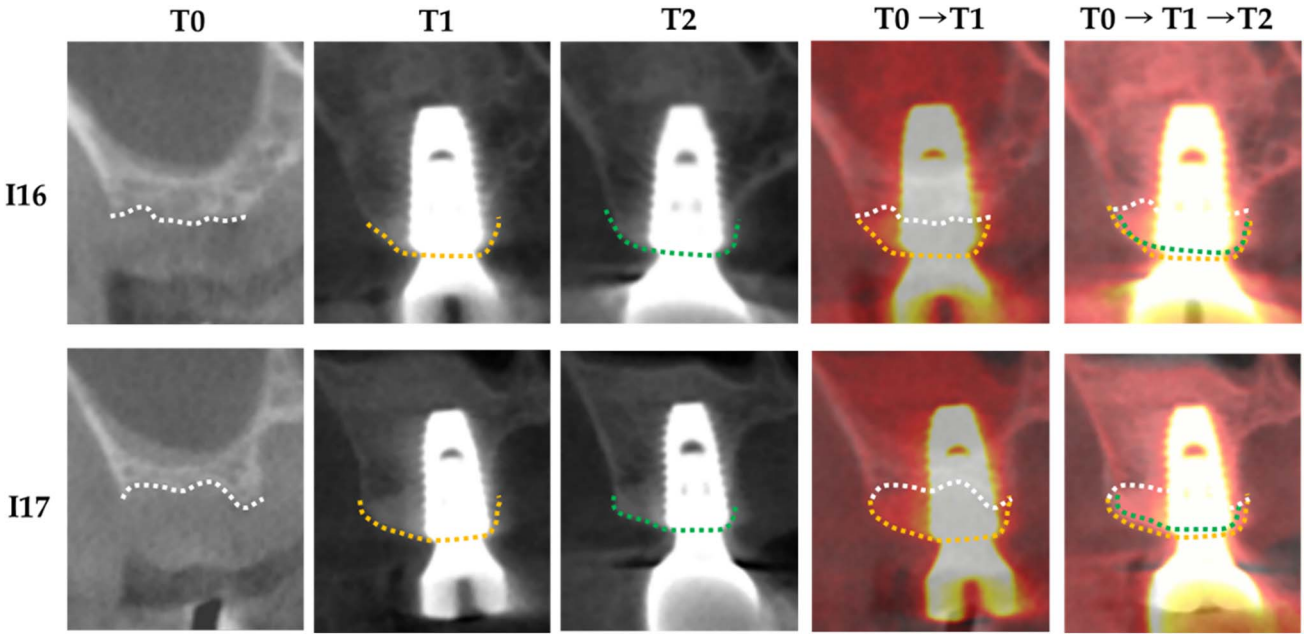

Figure 10. Cross-sectional images of case II; T0: preoperative; T1: immediately after surgery; T2: 1.5 years after surgery; preoperative crestal bone margin (black dotted line); augmented bone margin immediately after surgery (yellow dotted line); augmented bone margin 1.5 years after surgery (green line).

Conclusion

In conclusion, within the limitations of this work, vertical and horizontal augmentation in atrophic posterior maxilla can be performed successfully using the PCL mesh. The PCL mesh in this study seemed to be a safe biomaterial for clinical use. A further long-term randomized clinical trial is needed to validate its efficacy.

Abbreviations

3D: three-dimensional
CAD: computer-aided design
CAM: computer-aided manufacture
CBCT: cone-beam computerized tomography
GBR: guided bone regeneration
H1: the level at 1 mm below the implant platform
H2: the level at 2 mm below the implant platform
H3: the level at 3 mm below the implant platform
PCL: polycaprolactone
T0: baseline
T1: immediately postoperative
T2: the most recent follow up at 1.5–2 years

Acknowledgment

This research was supported by a grant of the Korea Health Technology R&D Project through the Korea Health Industry Development Institute (KHIDI), funded by the Ministry of Health & Welfare, Republic of Korea (grant number : HI22C1609).

References

1. Benic GI, Hammerle CH. Horizontal bone augmentation by means of guided bone regeneration. *Periodontol 2000*. 2014;66:13–40.

2. Urban IA, Montero E, Monje A, Sanz-Sanchez I. Effectiveness of vertical ridge augmentation interventions: a systematic review and meta-analysis. *J Clin Periodontol*. 2019;46(suppl 21):319–339.

3. Sanz-Sanchez I, Ortiz-Vigon A, Sanz-Martin I, Figuero E, Sanz M. Effectiveness of lateral bone augmentation on the alveolar crest dimension: a systematic review and meta-analysis. *J Dent Res*. 2015;94(suppl 9):128S–142S.

4. Thoma DS, Bienz SP, Figuero E, Jung RE, Sanz-Martin I. Efficacy of lateral bone augmentation performed simultaneously with dental implant placement: a systematic review and meta-analysis. *J Clin Periodontol*. 2019;46(suppl 21):257–276.

5. Benic GI, Thoma DS, Munoz F, Sanz Martin I, Jung RE, Hammerle CH. Guided bone regeneration of peri-implant defects with particulated and block xenogenic bone substitutes. *Clin Oral Implants Res*. 2016;27:567–576.

6. Mir-Mari J, Wui H, Jung RE, Hammerle CH, Benic GI. Influence of blinded wound closure on the volume stability of different GBR materials: an in vitro cone-beam computed tomographic examination. *Clin Oral Implants Res*. 2016;27:258–265.

7. Wang HL, Boyapati L. "PASS" principles for predictable bone regeneration. *Implant Dent*. 2006;15:8–17.

8. Sagheb K, Schiegnitz E, Moergel M, Walter C, Al-Nawas B, Wagner W. Clinical outcome of alveolar ridge augmentation with individualized CAD-CAM-produced titanium mesh. *Int J Implant Dent*. 2017;3:36.

9. Sumida T, Otawa N, Kamata YU, et al. Custom-made titanium devices as membranes for bone augmentation in implant treatment: clinical application and the comparison with conventional titanium mesh. *J Craniomaxillofac Surg*. 2015;43:2183–2188.

10. Zhou L, Su Y, Wang J, Wang J, Wang X, Liu Q. Effect of exposure rates with customized versus conventional titanium mesh on guided bone regeneration: a systematic review and meta-analysis. *J Oral Implantol*. 2021.

11. Chiapasco M, Casentini P, Tommasato G, Dellavia C, Del Fabbro M. Customized CAD/CAM titanium meshes for the guided bone regeneration of severe alveolar ridge defects: preliminary results of a retrospective clinical study in humans. *Clin Oral Implants Res*. 2021;32:498–510.

12. Sun H, Mei L, Song C, Cui X, Wang P. The in vivo degradation, absorption and excretion of PCL-based implant. *Biomaterials*. 2006;27:1735–1740.

13. Shim J-H, Won J-Y, Sung S-J, et al. Comparative efficacies of a 3D-printed PCL/PLGA/β-TCP membrane and a titanium membrane for guided bone regeneration in beagle dogs. *Polymers (Basel)*. 2015;7:2061–2077.

14. Seibert JS. Reconstruction of deformed, partially edentulous ridges, using full thickness onlay grafts. Part I. Technique and wound healing. *Compend Contin Educ Dent*. 1983;4:437–453.

15. Lee DH, Shin YH, Park JH, Shim JS, Shin SW, Lee JY. The reliability of Anycheck device related to healing abutment diameter. *J Adv Prosthodont*. 2020;12:83–88.

16. Lee JY, Park JY, Hong IP, et al. 3D-printed barrier membrane using mixture of polycaprolactone and beta-tricalcium phosphate for regeneration of rabbit calvarial defects. *Materials (Basel)*. 2021;14:3280.

17. Pae HC, Kang JH, Cha JK, et al. 3D-printed polycaprolactone scaffold mixed with beta-tricalcium phosphate as a bone regenerative material in rabbit calvarial defects. *J Biomed Mater Res B Appl Biomater*. 2019;107:1254–1263.

18. Shim JH, Won JY, Park JH, et al. Effects of 3D-printed polycaprolactone/beta-tricalcium phosphate membranes on guided bone regeneration. *Int J Mol Sci*. 2017;18:899.

19. Won JY, Park CY, Bae JH, et al. Evaluation of 3D printed PCL/PLGA/-beta-TCP versus collagen membranes for guided bone regeneration in a beagle implant model. *Biomed Mater*. 2016;11:055013.

20. Park JY, Jung IH, Kim YK, et al. Guided bone regeneration using 1-ethyl-3-(3-dimethylaminopropyl) carbodiimide (EDC)-cross-linked type-I collagen membrane with biphasic calcium phosphate at rabbit calvarial defects. *Biomater Res*. 2015;19:15.

21. Chuenjitkuntaworn B, Inrung W, Damrongsri D, Mekaapiruk K, Supaphol P, Pavasant P. Polycaprolactone/hydroxyapatite composite scaffolds: preparation, characterization, and in vitro and in vivo biological responses of human primary bone cells. *J Biomed Mater Res A*. 2010;94:241–251.

22. Omar O, Elgali I, Dahlin C, Thomsen P. Barrier membranes: more than the barrier effect? *J Clin Periodontol*. 2019;46(suppl 21):103–123.

23. Cucchi A, Sartori M, Aldini NN, Vignudelli E, Corinaldesi G. A proposal of pseudo-periosteum classification after GBR by means of titanium-reinforced d-PTFE membranes or titanium meshes plus cross-linked collagen membranes. *Int J Periodontics Restorative Dent*. 2019;39:e157–e165.

24. Corinaldesi G, Pieri F, Marchetti C, Fini M, Aldini NN, Giardino R. Histologic and histomorphometric evaluation of alveolar ridge augmentation using bone grafts and titanium micromesh in humans. *J Periodontol*. 2007;78:1477–1484.

25. Lim HC, Lee JS, Choi SH, Jung UW. The effect of overlaying titanium mesh with collagen membrane for ridge preservation. *J Periodontal Implant Sci*. 2015;45:128–135.